

Prospects of LIGO for constraining inclination of merging compact binaries associated with three-dimensionally localized short-hard GRBs

Naoki Seto

Department of Physics, and Astronomy, 4186 Frederick Reines Hall, University of California, Irvine, CA 92697

We study prospects of a method to constrain the inclination of a coalescing compact binary by detecting its gravitational waves associated with a three-dimensionally localized (direction and distance) short-hard gamma-ray burst. We take advantage of a synergy of these two observations, and our method can be applied even with a single interferometer. For a nearly face-on binary the inclination angle I can be constrained in the range $1 - SNR^{-1} \leq \cos I \leq 1$ (SNR : the signal to noise ratio of gravitational wave detection), provided that the error of the distance estimation is negligible. This method would help us to study properties of the short-hard bursts, including potentially collimated jet-like structures as indicated by recent observation.

I. INTRODUCTION

The gamma-ray bursts have been known to be divided into two classes, the long-soft bursts and the short-hard bursts (SHBs). While the former are likely to be produced at explosions of massive stars in star forming galaxies typically at high redshift $z \gtrsim 1$ [1], the nature of SHBs has been a long-standing mystery. However, recent discoveries of X-ray afterglows of SHBs by Swift and HETE satellites allowed us to localize them accurately and rapidly enough to specify their host galaxies and finally determine their distances [2, 3, 4, 5, 6].

One of them, GRB 050724 was found in an elliptical galaxy at $z = 0.257$ with an old stellar population [4], and GRB 050509b is likely to be in a similar galaxy at $z = 0.225$ [6]. While GRB 050709 was in a star forming galaxy at $z = 0.160$, its light curve excluded a supernova association [5]. These results support that coalescing compact binaries (double neutron stars (NS+NSs) or black hole-neutron star (BH+NS) systems) are the promising origins of SHBs [7], though the estimated typical age of these binaries for SHBs are longer than that of known NS+NSs in our galaxy [8, 9].

Coalescing compact binaries are also promising sources of gravitational radiation for LIGO and other ground-based interferometers [10]. A one year scientific run (S5) is ongoing with LIGO that has sensitivity to detect NS+NSs to ~ 15 Mpc [11]. Recent theoretical analysis predicts that the probability of a simultaneous detection of gravitational waves by LIGO and a SHB by Swift in one year is $\sim 30\%$ for BH-NS merger and $\sim 10\%$ for NS+NS (depending on the lower end of the luminosity function of SHBs) [9]. Therefore, we might soon experience the first detection of gravitational waves associated with a localized SHB.

The observed afterglows of two SHBs showed steeper power-law decays that indicate SHBs have collimated jet-like structures [5, 6], as found with long-soft bursts. The estimated beaming factor is ~ 0.03 for GRB 050709 [5] and ~ 0.01 for GRB 050724 [6]. Here we defined the beaming factor as the fraction of 4π steradians into which jets are emitted. This enabled us to estimate their total energies $\sim 3 \times 10^{48}$ erg that is smaller than the long-soft bursts by ~ 2 orders of magnitude. If a SHB is associated with a coalescing binary, it is likely that the orientation of the jet is aligned with the angular momentum of the binary that would be clearly imprinted on the observed gravitational waveform.

In this paper we propose a method with which the inclination of a binary will be interestingly constrained as a synergy of three-dimensional localization by electro-magnetic waves (EMWs) and observation of gravitational waves, even using a single interferometer. Therefore, LIGO could provide us an important geometrical information to understand properties of SHBs.

This paper is organized as follows: in §II we describe our method to estimate inclination of binaries with using a single gravitational wave interferometer. Expected error for our method is studied in §III. Then, in §IV, we extend our study for observation with multiple detectors, such as, LIGO-VIRGO network. Brief discussions are presented in §V.

II. GWS AND CONSTRAINT FOR INCLINATION

For simplicity we use the restricted post-Newtonian description [12] with neglecting precession induced by spin that might be important for BH-NS, but not for NS+NS [13] (see also [14] for recent analysis). The two polarization waveforms in the principle polarization coordinate are given as [12, 15]

$$h_+(t) = Bf^{2/3}(1 + V^2)\cos(\Phi(t)), \quad (1)$$

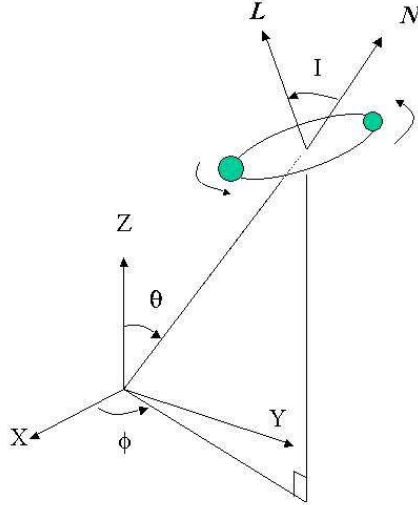


FIG. 1: Configuration of a binary and an interferometer (X and Y -axes; directions of its two arms). The unit vector \mathbf{N} represents the direction of the binary, and the unit vector \mathbf{L} is the orientation of its angular momentum. The angle I is the inclination with $\cos I = \mathbf{L} \cdot \mathbf{N} \equiv V$. The polarization angle ψ specifies the direction of \mathbf{L} around the vector \mathbf{N} .

$$h_{\times}(t) = Bf^{2/3}(2V) \sin(\Phi(t)), \quad (2)$$

where $\Phi(t) = 2\pi \int_{t_I}^t f(t', M_c, \dots, t_I) dt' + \varphi_c$ is the phase of the waves, and t_I and φ_c are constants. The parameter V is defined by

$$V \equiv \cos I \quad (3)$$

with the inclination angle I shown in figure 1, and is the primary target in this paper. The chirp mass M_c is the most important parameter to characterize the time evolution of the frequency $f = 1/2\pi d\Phi/dt$ and given by two (redshifted) masses of the binary as $M_c = m_1^{3/5} m_2^{3/5} (m_1 + m_2)^{-1/5}$. The intrinsic amplitude B at the quadruple order is given by the chirp mass M_c and the distance (more precisely, luminosity distance) r to the binary [10, 16],

$$B = 2 \frac{G^{5/3} M_c^{5/3} \pi^{2/3}}{rc^4}. \quad (4)$$

Response $h(t)$ of the interferometer to the two polarization modes is written in terms of the beam-pattern functions F_+ and F_{\times} as

$$h(t) = F_+ h_+(t) + F_{\times} h_{\times}(t). \quad (5)$$

The beam-pattern functions are determined by three angles θ , ϕ and ψ as [17]

$$F_+ = a_1 \cos 2\psi - a_2 \sin 2\psi, \quad (6)$$

$$F_{\times} = a_1 \sin 2\psi + a_2 \cos 2\psi \quad (7)$$

with $a_1 \equiv \frac{1}{2}(1 + \cos^2 \theta) \cos 2\phi$ and $a_2 \equiv \cos \theta \sin 2\phi$. The angles (θ, ϕ) represent the direction of the binary in the polar coordinate attached to the interferometer as in figure 1, and ψ is the polarization angle that fixes the axial direction of the vector \mathbf{L} around the direction \mathbf{N} (see *e.g.* figure 1 in [13]).

When we take Fourier transformation of the response $h(t)$, the result is formally given as

$$\hat{h}(f) = AR(V, \psi, \theta, \phi) f^{-7/6} \exp[i\Psi(f)]. \quad (8)$$

Here we used the stationary phase approximation, and the phase $\Psi(f)$ is a real function. The overall amplitude of the signal $AR(V, \psi, \theta, \phi)$ is given by [15]

$$R = \sqrt{\{(V^2 + 1)F_+\}^2 + (2VF_{\times})^2}, \quad (9)$$

TABLE I: Determination of $Q \equiv (AR)/AR_{max}$

notation	observation	error
A	M_c : GW (chirp)	~ 0
$(\propto M_c^{5/6}/r)$	r : EMW (localization)	$\Delta H_0/H_0$, velocity
(AR)	GW (amplitude)	$\sim (SNR)^{-1}$
R_{max}	(θ, ϕ) : EMW (localization)	~ 0

and

$$A = \sqrt{\frac{5}{96}} \frac{G^{5/6}}{\pi^{2/3} c^{3/2}} \frac{M_c^{5/6}}{r}. \quad (10)$$

The quantity R is a complicated function of four angular variables (I, ψ, θ, ϕ) , and we cannot solve them separately only with a single interferometer. Even if the direction (θ, ϕ) is known (*e.g.* from EMW observation), we need at least two not-aligned interferometers to solve V , ψ and r from observed amplitudes and the relative phases (see [18] and references therein).

Now we assume a situation that the three dimensional position (r, θ, ϕ) of a coalescing binary is determined through the afterglow of SHB associated with coalescing (ispiral) gravitational waves detected by LIGO. We start with the case for a single interferometer. With gravitational wave observation the chirp mass M_c can be determined well by the frequency evolution [16]. Thus we can estimate the intrinsic amplitude $A \propto M_c^{5/6}/r$ by combining the chirp mass and the distance r from EMW localization. From gravitational wave data we can also get the combination (AR) as the observed amplitude. We describe the method to constrain the parameter V by dealing with these observed quantities. Basic aspects are summarized in table 1. Firstly, we calculate the maximum value of $R(V, \psi, \theta, \phi)$ for the observed direction (θ, ϕ) of SHB. This is realized with the face-on configuration with $|V| = 1$. In this case the polarization angle ψ does not have meaning due to the symmetry of the geometry, and R_{max} is independent on ψ ,

$$R_{max} \equiv R(1, \psi, \theta, \phi). \quad (11)$$

Secondly, we take the ratio Q of the observed gravitational wave amplitude (AR) to the estimated combination $A \cdot R_{max}$ as

$$Q = \frac{(AR)}{A \cdot R_{max}} = \frac{R}{R_{max}}. \quad (12)$$

The ratio Q is written by

$$Q = \sqrt{\frac{1}{4}(1 + V^2)^2 \cos^2(2\psi + \gamma) + V^2 \sin^2(2\psi + \gamma)}. \quad (13)$$

with $\gamma = \arctan(a_2/a_1)$. This expression is valid also in the limit $(\theta, \phi) \rightarrow (\pi/2, \pi/4)$ where both the denominator and the numerator in eq.(12) vanish, as the interferometer becomes insensitive to the incident gravitational waves. In figure 2 we show the profile of Q with $\theta = \phi = 0$. The ratio Q takes a same value for $\pm V$ and, is periodic along the ψ -direction with period $\pi/2$. For a different combination (θ, ϕ) the profile Q in figure 2 shifts to the ψ -direction as characterized by the angle $\gamma/2$ in eq.(13). Therefore, without loss of generality, we can study the constraint on V for arbitrary (θ, ϕ) only using figure 2 with which the constrained region for V can be easily read with a given Q . Note that the modes higher than the quadrupole order might slightly change this contour map and also affect the estimation of the quadrupole amplitude A . These aspects are not peculiar to our method, but common to data analyses for gravitational wave astronomy for coalescing binaries.

For a given value of Q , the maximum of V is realized with the choice $\psi = 0$ in figure 2, and the minimum is with $\psi = \pi/4$. In figure 3 (solid curves) we show the constrained region for V as a function of Q . The upper curve is $V = Q$ and the lower one is $V = \sqrt{2Q - 1}$. Thus the parameter V is constrained by $\sqrt{\max(2Q - 1, 0)} \leq V \leq Q$. For the ratio Q close to 1, the binary must be almost face-on, as this is the only configuration to realize the maximum amplitude $Q = 1$. In contrast, for $Q \leq 1/2$, the parameter V can take the range $[0, Q]$. The allowed region for V is very small for $Q \sim 1$, when the binary is nearly face-on and SHB is expected to be luminous with collimated jet-like structures. Even with a smaller Q (*e.g.* $Q = 0.6$) we can correctly discriminate that the SHB is completely off-axis.

So far we have studied case with single interferometer. By using three widely separated interferometers the direction (θ, ϕ) of a binary can be determined from the time delays of the gravitational wave signals, and the angles (I, ψ) and

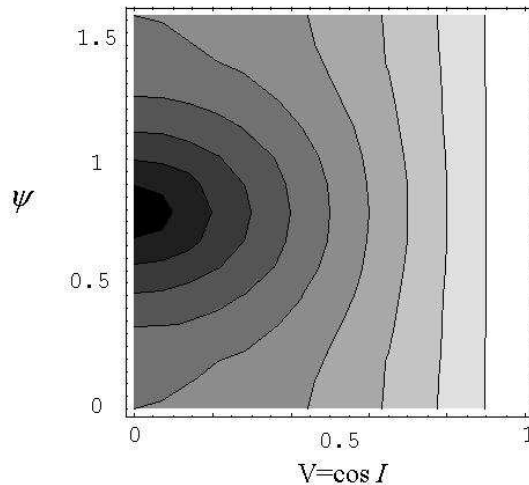


FIG. 2: The contour plot for Q as a function of V and ψ with $\theta = 0$ and $\phi = 0$. Contour levels correspond to 0.1 (black) to 0.9 (white). Q is periodic along ψ -direction with period $\pi/2$, and $Q = 1$ for $V = 1$ (face-on configuration). The contour plot Q shifts to ψ -direction for different combinations (θ, ϕ) .

the distance r can be also estimated only from gravitational wave observation [12]. As commented earlier, we can, in principle, solve two orientation angles (I, ψ) and the distance r by using two not-aligned interferometers for a binary with known direction. We will see this in §IV.

LIGO has essentially two interferometers. One is at Hanford, Washington, and another is at Livingston, Louisiana. While the separation between them is $\sim 3000\text{km}$ (corresponding to $\sim 27^\circ$ measured from the center of the earth), they are nearly parallel to increase correlation of burst signals [12]. As a result, it is not easy to observe two polarization modes separately and thereby estimate the parameter $V = \cos I$ well with using two LIGO interferometers, compared with using combination such as LIGO-VIRGO network. In §IV we will return to analyses with multiple interferometers. But our studies for a single interferometer would provide rough outlook for determination of the inclination with nearly aligned interferometers as LIGO.

III. OBSERVATIONAL ERROR

In actual observation, we cannot determine the ratio Q without error ΔQ . Here we analyze its effects for constraining V . As we discussed, the ratio is obtained by three observed values A , R_{max} and (AR) (see table 1). We can formally write down the relative error for Q as

$$\frac{\Delta Q}{Q} = \frac{\Delta(AR)}{(AR)} + \frac{\Delta A}{A} + \frac{\Delta R_{max}}{R_{max}}. \quad (14)$$

We are dealing with a situation when the afterglow of SHB is observed and the direction (θ, ϕ) is determined very well (*e.g.* $\lesssim 1\text{arcsec}$ level). Therefore, the term $\Delta R_{max}/R_{max}$ is negligible compared with other two terms.

If the orbital precession of the binary is not significant, the estimation error for the observed gravitational wave amplitude (AR) has little correlation with errors for other parameters related to the phase, such as, the chirp mass. Thus we have

$$\frac{\Delta(AR)}{(AR)} \simeq (SNR)^{-1} \quad (15)$$

with SNR being the signal to noise ratio for the detected gravitational wave signal [12]. The typical detection threshold for a coalescing binary is ~ 8 . If we use the temporal information from the observed SHB, the threshold somewhat decreases (but less than a factor of 2) [20].

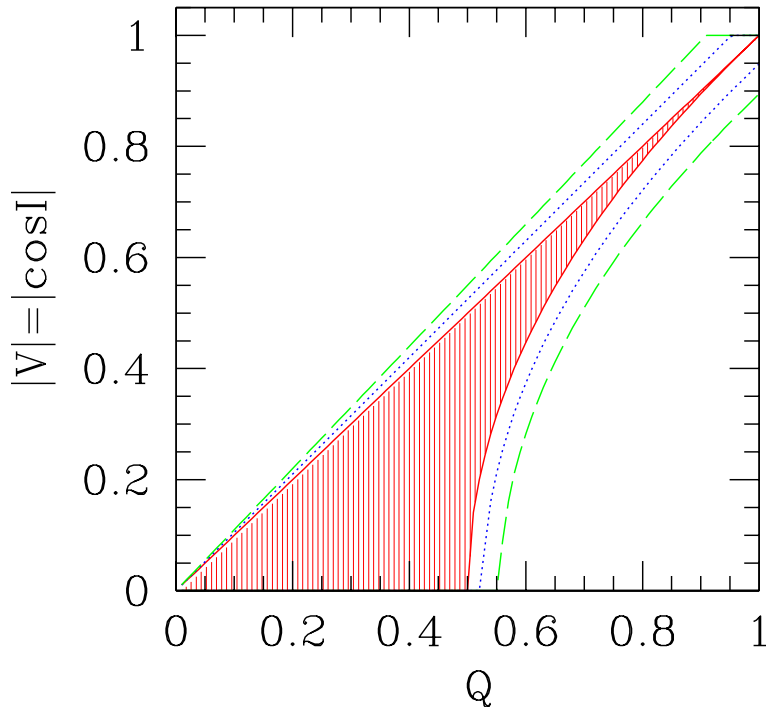


FIG. 3: Constraint for $V = \cos I$ with given ratio Q . Without error $\Delta Q = 0$, the parameter V must be within the shaded region determined by two solid curves $V = Q$ and $V = \sqrt{\max(2Q - 1, 0)}$. These two curves are obtained by cutting the surface in figure 2 along $\psi = 0$ and $\psi = \pi/4$. The dotted curves show the allowed region with 5% error for Q ($\Delta Q/Q = 0.05$), and the dashed curves show the region with 10% error ($\Delta Q/Q = 0.10$). With a nearly face-on configuration we have $\Delta V \in [1 - \Delta Q, 1]$.

For the intrinsic amplitude A we need the distance r from EMW observation and the chirp mass M_c from gravitational wave data. The latter can be determined very accurately, as it is the primary parameter for the time evolution of the gravitational wave phase whose information is crucial for detecting gravitational waves with matched filtering method [10, 16]. In this paper we neglect estimation error for chirp mass. Under this prescription our results do not depend on the order of the post-Newtonian expansion in the restricted post-Newtonian approach without orbital precession. For a very nearby SHB we might estimate its distance r with various astronomical data. If we use the redshift-distance relation (Hubble law; $r = cz/H_0$ at low redshift) to convert its observed redshift z to the distance r , the estimated distance r might be significantly contaminated by the peculiar velocity of the host galaxy. At distance $r \sim 300\text{Mpc}$ (NS+NSs detectable with LIGOII) the uncertainty of the Hubble parameter H_0 could be a problem, but those of other cosmological parameters (*e.g.* the density parameter Ω_0) would not be important at these distances. The recently reported value $H_0 = 71^{+4}_{-3}\text{km/sec/Mpc}$ by WMAP team [21] contains $\sim 5\%$ error. As the distance error would be the dominate source of the error ΔA , we have

$$\frac{\Delta A}{A} \simeq \frac{\Delta r}{r}. \quad (16)$$

The error for the estimation of the gravitational wave amplitude (AR) and the distance r from EMW observation would be independent. Then, using eqs.(14)(15)(24) and putting $\Delta R_{max}/R_{max} = 0$, the typical value for relative rms error of Q is given as

$$\frac{\Delta Q_{rms}}{Q} \simeq \sqrt{\left(\frac{1}{SNR}\right)^2 + \left(\frac{\Delta r}{r}\right)^2} \quad (\text{typical case}). \quad (17)$$

Next we study how the estimation error ΔQ changes the allowed region for V . For a given Q we expand its possible value in the band $[\max(0, Q - \Delta Q), \min(1, Q + \Delta Q)]$ and solve corresponding V in (V, ψ) -plane (figure 2). Then we

obtain the following result

$$\sqrt{\max\{2(Q - \Delta Q) - 1, 0\}} \leq V \leq \min(1, Q + \Delta Q). \quad (18)$$

In figure 3 we added the allowed region for V from the observed value Q whose relative error is $\Delta Q/Q = 0.05$ (dotted curves) and 0.10 (dashed curves). For a almost face-on binary ($1 - V \ll 1$), we have $V \in [1 - \Delta Q, 1]$. With signal to noise ratio $SNR \sim 10$ and the distance error less than 5%, the constraint becomes $V \in [0.87, 1]$.

IV. MULTIPLE DETECTORS

A. Solving degeneracy

In this subsection we discuss observational analysis to estimate the inclination V separately from the polarization direction ψ with using networks of detectors. Following Ref.[12] we introduce two functions $\sigma(\mathbf{N})$ and $\epsilon(\mathbf{N})$ that characterize sensitivity of a network to gravitational waves with various directions and polarizations. As concrete examples of networks, we consider the following three combinations; (i) LIGO-Hanford (4km), LIGO-Livingston and VIRGO, (ii) LIGO-Hanford (4km) and VIRGO, (iii) LIGO-Hanford (4km) and LIGO-Livingston. The total numbers of detectors N_d are three for case (i) and two for cases (ii) and (iii). For simplicity we assume that all detectors have identical sensitivity. The total signal to noise ratio for a binary with directional vectors (\mathbf{N}, \mathbf{L}) , distance r and a fixed chirp mass is written as

$$SNR_{tot}^2 = \frac{r_0^2}{r^2} \sigma(\mathbf{N}) [c_0(V) + \epsilon(\mathbf{N})c_1(V) \cos(4\bar{\psi})], \quad (19)$$

where $\bar{\psi}$ is the polarization angle of the binary angular momentum \mathbf{L} measured from a preferred direction that is determined by configuration of each network and also fixes two orthogonal polarization bases in the present analysis. The combination r_0/r represents the signal to noise ratio of single detector for a face-on ($|V| = 1$) binary at perpendicular direction to the detector plane ($\theta = 0$ in figure 1). For a binary neutron stars with chirp mass $1.2M_\odot$ the distance r_0 corresponds to ~ 5000 Mpc for advanced LIGO. Here we used numerical results given in [22] based on the noise curve for advanced LIGO with its wide band setting [23]. Using relative sensitivities of LIGO and advanced LIGO to double neutron stars (*e.g.* [24]), the distance r_0 for LIGO is ~ 320 Mpc. Note that these distances are for $SNR = 1$ with an optimal configuration of a binary and a single interferometer.

The function $\sigma(\mathbf{N})$ shows sensitivity of a network to gravitational wave from direction \mathbf{N} with averaged polarization, and generally takes values in $0 \leq \sigma(\mathbf{N}) \leq N_d/2$ (N_d : number of detectors with identical sensitivity). For our three networks its maximum value is 1.04 for case (i), 0.65 for case (ii) and 0.94 for case (iii), while its minimum value is 0.148, 0.118 and 0.0040 respectively. As two LIGO detectors are nearly aligned, they are not effectively complimentary to decrease the blind directions with $\sigma(\mathbf{N}) \ll 1$.

The function $\epsilon(\mathbf{N})$ ($0 \leq \epsilon \leq 1$) represents asymmetry of a network with respect to its sensitivity to two orthogonal polarization modes coming from direction \mathbf{N} . For a direction \mathbf{N} with $\epsilon(\mathbf{N}) \sim 1$ a network is sensitive only to one polarization mode, while two modes are measured with a similar sensitivity for $\epsilon(\mathbf{N}) \sim 0$. With a single detector we identically have $\epsilon(\mathbf{N}) = 1$. For our three networks, this parameter can take the maximum value $\epsilon(\mathbf{N}) = 1$ for some directions.

In eq.(19) two functions $c_0(V)$ and $c_1(V)$ are defined by

$$c_0(V) = \frac{(1 + V^2)^2}{4} + V^2, \quad c_1(V) = \frac{(1 + V^2)^2}{4} - V^2. \quad (20)$$

For a face-on binary with $|V| = 1$, we have $c_1 = 0$ and the expression (19) does not depend on the polarization angle $\bar{\psi}$, as expected.

Next we evaluate magnitudes of estimation errors $\Delta\alpha_i$ for fitting parameters $\alpha_i = (r, V, \bar{\psi})$ that are related to amplitude of the gravitational waveform. We use the Fisher matrix approach that basically uses linear responses of the waveform to variations of fitting parameters. In other words, the first derivatives of the waveform by the fitting parameters are used to evaluate the expected errors. Under this approach, correlation between the parameters α_i and those related to frequency evolution are practically negligible in the restricted post-Newtonian approach [12].

With using eqs.(4.38) and (4.39) in Ref.[12] and integrating out the information of the phase constant φ_c (see arguments following eq.(2)), the covariance of estimation errors for parameters $(r, V, \bar{\psi})$ are given as

$$\langle \Delta\bar{\psi} \Delta\bar{\psi} \rangle = E [1 + 6V^2 + V^4 + (1 - V^2)^2 \epsilon(\mathbf{N}) \cos(4\bar{\psi})] / (1 - V^2)^2 \quad (21)$$

$$\langle \Delta \bar{\psi} \Delta r \rangle = -2Er\epsilon(\mathbf{N}) \sin(4\bar{\psi}) \quad (22)$$

$$\langle \Delta \bar{\psi} \Delta V \rangle = 0 \quad (23)$$

$$\langle \Delta r \Delta r \rangle = 4Er^2(1 + V^2 - (1 - V^2)\epsilon(\mathbf{N}) \cos(4\bar{\psi})) \quad (24)$$

$$\langle \Delta r \Delta V \rangle = 2ErV(3 + V^2 - (1 - V^2)\epsilon(\mathbf{N}) \cos(4\bar{\psi})) \quad (25)$$

$$\langle \Delta V \Delta V \rangle = E [1 + 6V^2 + V^4 + \epsilon(\mathbf{N}) \cos(4\bar{\psi})(1 - V^2)^2] \quad (26)$$

with

$$E = \frac{r^2}{r_o^2 \sigma(\mathbf{N})(1 - \epsilon(\mathbf{N})^2)(1 - V^2)^2}. \quad (27)$$

Equation (24) for the distance error is same as eq.(4.41) in Ref.[12]. In the next subsection we will compare the estimation errors for the inclination under various situations, and hereafter, we denote the expression (26) as $\langle \Delta V \Delta V \rangle_N$ for notational clarity. The errors become large for binaries close to face-on through the denominator of the factor E . This is because the derivatives of the gravitational waveform with respect to the parameters r and V become linearly dependent at $|V| = 1$, and they are degenerated at parameter fitting [19]. In the same manner the error becomes large for sky directions with $\epsilon(\mathbf{N}) \sim 1$, as we can measure only one polarization mode that are not enough to determine parameters $(r, V, \bar{\psi})$ separately. However, without depending on the values $\epsilon(\mathbf{N})$ and V , the combination $SNR_{tot} \propto [(c_0(V) + \epsilon(\mathbf{N})c_1(\mathbf{N}) \cos(4\bar{\psi}))^{1/2}/r]$ can be determined well and its error is given only by the total signal to noise ratio as $\Delta(SNR_{tot})/(SNR_{tot}) = (SNR_{tot})^{-1}$. The situation is same as in the previous sections for single detector. We can also confirm this with directly using equations from (21) to (27).

Now we study the case that the distance r to a binary is given from EMW observation, assuming its error is negligible. After straightforward calculation with eqs. (21) to (27), the estimation errors for parameters $(\bar{\psi}, V)$ are given by a 2×2 Fisher matrix, and the $V - V$ component becomes

$$\langle \Delta V \Delta V \rangle_r = \frac{r^2(1 - \epsilon(\mathbf{N})^2 \cos^2(4\bar{\psi}))}{r_o^2 \sigma(\mathbf{N})(1 - \epsilon(\mathbf{N})^2)(1 + V^2 - \cos(4\bar{\psi})\epsilon(\mathbf{N})(1 - V^2))}. \quad (28)$$

Here the suffix r represents the condition that the distance r of the binary is given. Note that the singular behavior at $|V| = 1$ disappeared. This is because we do not need to solve r and V simultaneously only from gravitational wave observation. However, the error $\langle \Delta V \Delta V \rangle_r^{1/2}$ for the inclination still becomes large with $\epsilon \rightarrow 1$. To deal with the situation we introduce a new parameter \mathcal{Q} defined by

$$\mathcal{Q} \equiv \frac{AR_{tot}}{AR_{max}} = \left(\frac{c_0(V) + \epsilon(\mathbf{N})c_1(V) \cos(4\bar{\psi})}{c_0(1) + \epsilon(\mathbf{N})c_1(1) \cos(4\bar{\psi})} \right)^{1/2} = \left(\frac{c_0(V) + \epsilon(\mathbf{N})c_1(V) \cos(4\bar{\psi})}{2} \right)^{1/2}, \quad (29)$$

and change variables from $(\bar{\psi}, V)$ to (\mathcal{Q}, V) . The parameter \mathcal{Q} for multiple detectors is a simple generalization of the previous parameter Q in eq.(12) defined for single detector. In figure 4 we show the allowed region of the combination (\mathcal{Q}, V) for given network parameter ϵ . For a direction with $\epsilon = 1$ the allowed region coincides with that for $Q-V$ given by the shaded region in figure 3. When we decrease ϵ form 1 to 0, the region shrinks as in figure 4, and it becomes a single curve $\mathcal{Q} = (c_0(V)/2)^{1/2}$ at $\epsilon = 0$.

Next we consider a Gaussian probability distribution function (PDF) $P(\mathcal{Q}_x, V_x | \mathcal{Q}, V)$ of the estimated parameters (\mathcal{Q}_x, V_x) around their true values (\mathcal{Q}, V) . We calculate the covariances of errors for parameters (\mathcal{Q}, V) by using the 2×2 Fisher matrix for the original combination $(\bar{\psi}, V)$. Even if the error $\langle \Delta V \Delta V \rangle_r^{1/2}$ is large at $\epsilon(\mathbf{N}) \sim 1$ as shown in eq.(28), the parameter \mathcal{Q} can be estimated relatively well, as in the case for single detector. For example, with a $1 - \sigma$ error ellipsoid that is stretched toward V -direction as shown in figure 4, we can estimate the inclination V much better by limiting the combination (\mathcal{Q}_x, V_x) into its allowed region discussed above. This difference shows one of potential problems of a simple evaluation based on Fisher matrix without dealing with global domain of the fitting parameters. Therefore, we define a new PDF $P_C(\mathcal{Q}_x, V_x | \mathcal{Q}, V)$ with the following two steps. We firstly narrow the parameter space (\mathcal{Q}_x, V_x) of the original Gaussian distribution $P(\mathcal{Q}_x, V_x | \mathcal{Q}, V)$ using the $\mathcal{Q}-V$ constraint in figure 4, and secondly renormalize the PDF appropriately. Then we calculate the estimation error $\langle \Delta V \Delta V \rangle_C$ as

$$\langle \Delta V \Delta V \rangle_C = \int dV_x d\mathcal{Q}_x P_C(\mathcal{Q}_x, V_x | \mathcal{Q}, V) (V_x - V)^2. \quad (30)$$

Here the suffix C represents to use the constraint.

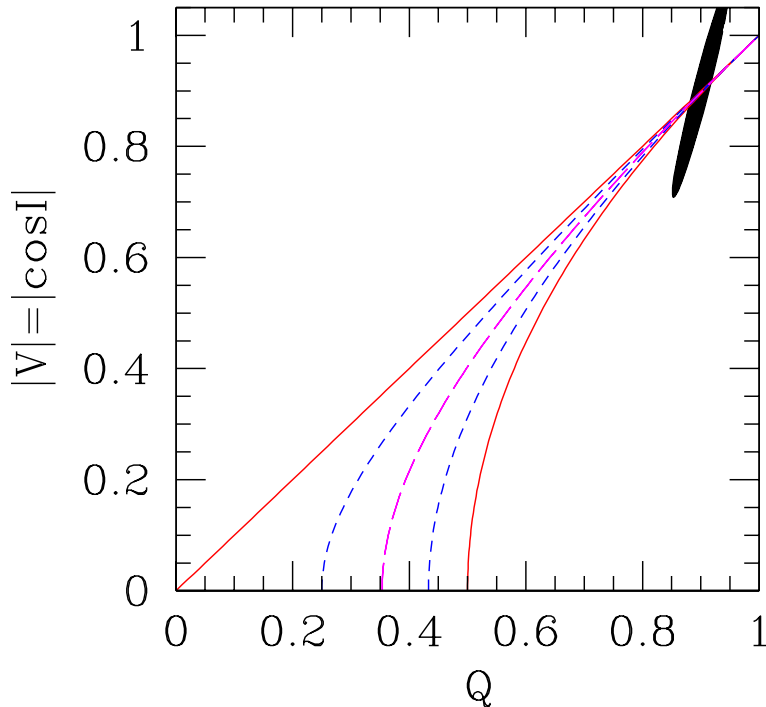


FIG. 4: Constraints for V and Q for given parameter $\epsilon(N)$ that represents asymmetry of the sensitivity of a network to two polarization modes coming from direction N . For $\epsilon = 1$ the combination (Q, V) is in the region bounded by two solid curves. This region is same as the shaded region in figure 3 for single detector. The short-dashed curves are for the boundary of the allowed region $\epsilon = 0.5$. For $\epsilon = 0$ the allowed region is on the long-dashed line $Q = [c_0(V)/2]^{1/2}$. The long ellipsoid around $(Q, V) = (0.9, 0.9)$ is an example of $1 - \sigma$ error ellipsoid described in the main text.

B. Monte Carlo analysis

In this subsection we compare estimations errors ΔV given by $\langle \Delta V \Delta V \rangle_N^{1/2}$, $\langle \Delta V \Delta V \rangle_r^{1/2}$ and $\langle \Delta V \Delta V \rangle_C^{1/2}$ presented in the previous subsection. The first one $\langle \Delta V \Delta V \rangle_N^{1/2}$ is the prediction by Fisher matrix for a binary whose distance is not given from EMW observation. The second one $\langle \Delta V \Delta V \rangle_r^{1/2}$ is also predicted by Fisher matrix but for binaries with known distances. For the third one we apply the Q - V constraint to binaries with known distances. For each network (i)-(iii) we prepare sample of “detectable binaries” with $SNR_{tot} \geq 8$ in the following manner. From eq.(19) the maximum distance r_{max} of binaries with the threshold $SNR_{tot} = 8$ is given as $r_{max} = r_0 [2 \max \sigma(N)]^{1/2} / 8$. A binary with $SNR_{tot} \geq 8$ must be in a sphere with radius r_{max} around the Earth, since this distance r_{max} is given for optimal configuration. In this sphere we put a binary with random position and orientation. If its SNR_{tot} is larger than 8, we add it to our sample of “detectable binaries”. We continue this until the total number of our sample becomes 200 for each network (i)-(iii).

We find that, out of these samples, the numbers of binaries with $|V| > 0.8$ are 102 for case (i), 99 for case (ii) and 101 for case (iii). For binaries with $|V| > 0.9$ we have 64, 62 and 60 respectively. While the intrinsic distribution of the parameter $|V|$ is homogeneous in the range $[0, 1]$ with random direction N and orientation L , our “detectable binaries” have skewed distributions of $|V|$ after selected with a signal-to-noise threshold.

In figure 5 we show the distribution of the estimation errors ΔV for case (i). The upper panel shows the results for all 200 binaries and the lower panel is only for 102 binaries with $|V| > 0.8$. Similar results are given in figs. 6 and 7 for cases (ii) and (iii). Comparing distributions for two Fisher matrix predictions $\langle \Delta V \Delta V \rangle_r^{1/2}$ (dashed curves) and $\langle \Delta V \Delta V \rangle_N^{1/2}$ (dotted curves), it is apparent that the estimation of the parameter V is significantly improved, if the distance r to the binary is determined by EMW observation. The differences between two curves become larger for

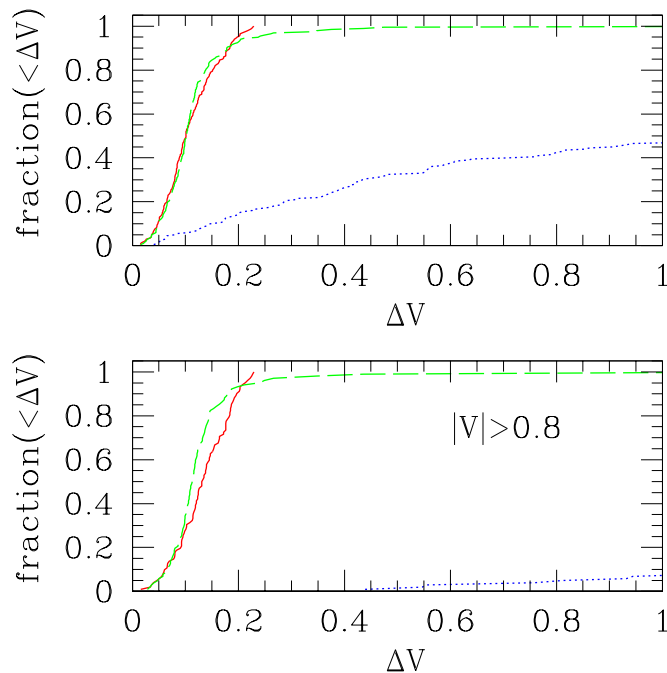


FIG. 5: cumulative distribution of the estimation errors ΔV for binaries with using two LIGO and VIRGO detectors (case (i)). The solid curves are results for $\langle \Delta V \Delta V \rangle_C^{1/2}$ (known distance from EMW observation and \mathcal{Q} - V constraint). The dashed curves are given by the Fisher matrix approach $\langle \Delta V \Delta V \rangle_r^{1/2}$ (known distance from EMW observation). The dotted curves are for $\langle \Delta V \Delta V \rangle_N^{1/2}$ (unknown distance from EMW observation). The lower panel is for binaries with $|V| > 0.8$.

subsample with $|V| > 0.8$ due to the degeneracy for the parameter fitting at the face on limit $|V| \rightarrow 1$.

We can study the effects of the \mathcal{Q} - V constraint with solid curves and dashed curves in figs.5-7. Note that this constraint does not always decrease the estimation error ΔV , as shown in figs. 5 and 6. However, the tail of large ΔV are removed by the constraint. As a result, the error ΔV becomes smaller than ~ 0.25 for our samples. The tails are mainly made by binaries with $\epsilon \sim 1$ for which it is difficult to observe two independent polarization modes and thereby solve two parameters $(V, \bar{\psi})$ separately. The constraint works well especially for case (iii) with two LIGO detectors whose orientations are nearly aligned. In this case the situation is similar to the observation with using a single detector as studied in §2. In the lower panel of figure 7 the median value of the error ΔV is reduced by $\sim 40\%$ by using the constraint. This indicate that we should be careful to use a simple Fisher matrix approach for evaluating the parameter estimation error for inclination.

V. DISCUSSIONS

We discussed prospects of a method to constrain the inclination angle of a coalescing compact binary by detecting its gravitational waves associated with a three-dimensionally localized SHB. With this method we can get an important geometrical information to understand the properties of SHBs and their afterglows as a function of the viewing angles of the jets (see *e.g.* [25] for long-soft bursts). We should comment that there would be a selection effect toward larger $|V|$ for a simultaneous detection of gravitational waves and SHB. This is because the observed gravitational wave amplitude would be larger (see §IV.B) and the SHB would be also luminous with the face-on configuration [9, 20].

By analyzing nearby samples with our method we might establish an efficient empirical criteria to select almost face-on binaries using observed properties of EMW signals. Then we can study cosmological parameters with face-on binaries at relatively high redshift where cosmological effects beyond the Hubble-law become important. The following is the outline of this approach. We first obtain the intrinsic amplitudes A by putting $R = R_{max}$ for the observed gravitational wave amplitude (AR) for binaries that are likely to be nearly face-on according to the empirical

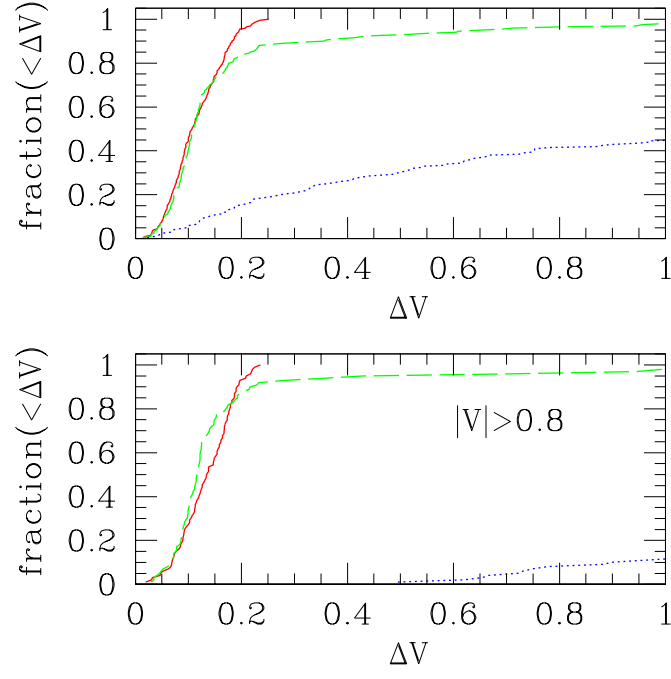


FIG. 6: Same as figure 4 with LIGO-Hanford and VIRGO detectors (case (ii)).

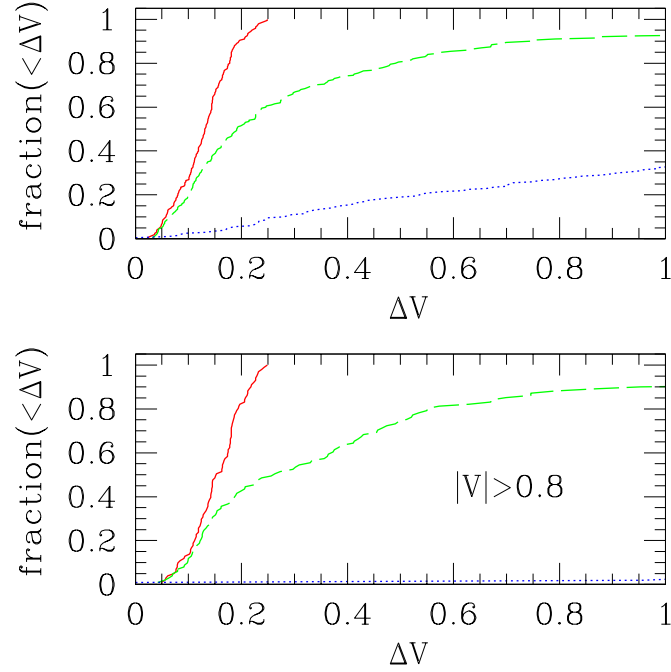


FIG. 7: Same as figure 4 with two LIGO detectors (case (iii)).

criteria. Then the luminosity distances r are obtained from eq.(10) and the estimated chirp masses. In this manner we might observationally study the redshift-distance relation with the redshift information naturally obtained from identified host galaxies with EMW observation. Note that this argument to estimate the distance r is different from the previous method in this paper to constrain the inclination angle by simply converting the observed redshift to the distance r for nearby binaries. Considering the strong correlation between the inclination V and the distance r for parameter estimation [12], this could be a powerful approach to investigate the dark energy with future gravitational wave detectors that can detect compact binaries at $z \sim 1$ (see also [16, 22, 26]).

Acknowledgments

The author would like to thank the referee for helpful comments to improve the draft. He also thanks H. Takahashi for useful conversations. This research was funded by McCue Fund at the Center for Cosmology, UC Irvine.

-
- [1] B. Zhang and P. Meszaros, *Int. J. Mod. Phys. A* **19**, 2385 (2004) [arXiv:astro-ph/0311321].
 - [2] N. Gehrels *et al.*, *Nature* **437**, 851 (2005); J. Bloom *et al.*, arXiv:astro-ph/0505480.
 - [3] J. S. Villasenor *et al.*, *Nature* **437**, 855 (2005).
 - [4] J. Hjorth *et al.*, *Nature* **437**, 859 (2005).
 - [5] D. B. Fox *et al.*, *Nature* **437**, 845 (2005).
 - [6] E. Berger *et al.*, arXiv:astro-ph/0508115.
 - [7] D. Eichler *et al.*, *Nature* **340**, 126 (1989).
 - [8] D. Guetta and T. Piran, arXiv:astro-ph/0511239.
 - [9] E. Nakar, A. Gal-Yam and D. B. Fox, arXiv:astro-ph/0511254.
 - [10] K. S. Thorne, in *Three hundred years of gravitation*, edited by S. W. Hawking and W. Israel (Cambridge University Press, Cambridge, 1987), pp. 330–458.
 - [11] <http://www.ligo.org/>
 - [12] C. Cutler and E. E. Flanagan, *Phys. Rev. D* **49**, 2658 (1994) [arXiv:gr-qc/9402014].
 - [13] T. A. Apostolatos *et al.*, *Phys. Rev. D* **49**, 6274 (1994).
 - [14] A. Buonanno *et al.* *Phys. Rev. D* **72**, 084027 (2005).
 - [15] P. Jaranowski, K. D. Kokkotas, A. Królak, and G. Tsegas, *Classical and Quantum Gravity*, **13**, 1279 (1996).
 - [16] B. F. Schutz, *Nature* **323** (1986) 310.
 - [17] F. P. Estabrook, *Gen. Rel. and Grav.* **17**, 719 (1985).
 - [18] S. Kobayashi and P. Meszaros, *Astrophys. J.* **585**, L89 (2003) [arXiv:astro-ph/0212539].
 - [19] D. Markovic, *Phys. Rev. D* **48**, 4738 (1993).
 - [20] C. S. Kochanek and T. Piran, *Astrophys. J.* **417**, L17 (1993) [arXiv:astro-ph/9305015].
 - [21] D. N. Spergel *et al.* [WMAP Collaboration], *Astrophys. J. Suppl.* **148**, 175 (2003) [arXiv:astro-ph/0302209].
 - [22] N. Dalal, D. E. Holz, S. A. Hughes and B. Jain, arXiv:astro-ph/0601275.
 - [23] E. Gustafson, D. Shoemaker, K. Strain and R. Weiss, 1999, LSC White Paper on Detector Research and Development (LIGO project document T990080-00-D).
 - [24] C. Cutler and K. S. Thorne, arXiv:gr-qc/0204090.
 - [25] R. Yamazaki, K. Ioka and T. Nakamura, *Astrophys. J.* **607**, L103 (2004) [arXiv:astro-ph/0401142].
 - [26] L. S. Finn, *Phys. Rev. D* **53**, 2878 (1996) [arXiv:gr-qc/9601048]; D. E. Holz and S. A. Hughes, *Astrophys. J.* **629**, 15 (2005) [arXiv:astro-ph/0504616].